

Flammability of In-Service Aircraft Thermal Acoustic Insulation Blankets

February 2010

DOT/FAA/AR-TN09/43

This document is available to the U.S. public through the National Technical Information Service (NTIS), Springfield, Virginia 22161.



U.S. Department of Transportation
Federal Aviation Administration

NOTICE

This document is disseminated under the sponsorship of the U.S. Department of Transportation in the interest of information exchange. The United States Government assumes no liability for the contents or use thereof. The United States Government does not endorse products or manufacturers. Trade or manufacturer's names appear herein solely because they are considered essential to the objective of this report. This document does not constitute FAA certification policy. Consult your local FAA aircraft certification office as to its use.

This report is available at the Federal Aviation Administration William J. Hughes Technical Center's Full-Text Technical Reports page: actlibrary.act.faa.gov in Adobe Acrobat portable document format (PDF).

1. Report No. DOT/FAA/AR-TN09/43		2. Government Accession No.		3. Recipient's Catalog No.	
4. Title and Subtitle FLAMMABILITY OF IN-SERVICE AIRCRAFT THERMAL ACOUSTIC INSULATION BLANKETS				5. Report Date February 2010	
				6. Performing Organization Code	
7. Author(s) Richard E. Lyon, Natallia Safronava*, Patricia Cahill, and Brian Conover*				8. Performing Organization Report No.	
9. Performing Organization Name and Address Federal Aviation Administration William J. Hughes Technical Center Airport and Aircraft Safety Research and Development Division Fire Safety Branch Atlantic City International Airport, NJ 08405 *SRA International, Inc. 1201 New Road, Suite 242 Linwood, NJ 08221				10. Work Unit No. (TRAVIS)	
				11. Contract or Grant No.	
12. Sponsoring Agency Name and Address U.S. Department of Transportation Federal Aviation Administration Air Traffic Organization NextGen & Operations Planning Office of Research and Technology Development Washington, DC 20591				13. Type of Report and Period Covered Technical Note	
				14. Sponsoring Agency Code AAI-100	
15. Supplementary Notes					
16. Abstract <p>Thermal acoustic insulation blankets are widely used in commercial aircraft to provide thermal insulation and acoustic damping. This report examines the burning effects on the thermal acoustic insulation blankets retrieved from the EVA Airways Flight BR67 fire event. On February 23, 2008, passengers disembarking from EVA Airways Flight BR67 reported smoke in the cabin of the Boeing 747-400 after landing at Suvamabhumi International Airport in Bangkok, Thailand. An investigation of the incident revealed burned thermal acoustic insulation blankets. The level of contamination on the encapsulating films of the as-received insulation blankets varied greatly. Samples of the contaminated film from different locations were weighed to determine the areal weight of contamination, were ranked by visual inspection, and were characterized by microscale combustion calorimetry to determine the thermal combustion properties. Thermal acoustic insulation blankets were also tested for flammability as prescribed by Title 14 Code of Federal Regulations 25.853 and 25.855. It was found that the visible contamination ranged in areal weight up to 167 grams per square meter of film surface and had a heat of combustion of 13 kJ/g, which is half that of the underlying insulation bag film. All in-service blankets and film samples passed the required 12-second vertical Bunsen burner test for flame resistance. The contaminated blankets did not pass the voluntary guideline for flame spread. Numerical modeling of the burning rate of contaminated blankets was conducted to help explain the flame spread results.</p>					
17. Key Words Heat of combustion, Microscale combustion calorimetry, Thermal acoustic insulation, Contamination, In-service aircraft			18. Distribution Statement This document is available to the U.S. public through the National Technical Information Service (NTIS), Springfield, Virginia 22161.		
19. Security Classif. (of this report) Unclassified		20. Security Classif. (of this page) Unclassified		21. No. of Pages 40	22. Price

TABLE OF CONTENTS

	Page
EXECUTIVE SUMMARY	vii
INTRODUCTION	1
MATERIALS	2
METHODS	3
Level of Contamination by Visual Inspection	3
Gravimetric Determination of Level of Contamination	4
Combustion Properties of In-Service Films by Microscale Combustion Calorimetry	4
Specific Heat Release Rate (Q)	5
Heat Release Capacity (η)	5
Pyrolysis Residue (μ)	5
Specific Heat of Combustion of the Specimen (h)	5
Specific Heat of Combustion of the Specimen Gases (h_g)	5
Areal Weight of Film Specimen (W_A)	5
Areal Weight of Film (W_f)	5
Areal Weight of Contamination (W_c)	6
Fire Load	6
Areal Heat Release Rate	6
Flame Resistance Test for Thermal Acoustic Insulation Blanket	6
Thermal Acoustic Insulation Blankets Flame Spread Tests	6
Numerical Modeling of Burning Rate of Insulation Blankets	6
Surface Contamination	7
Encapsulating Film	7
Fiberglass Insulation	7
RESULTS AND DISCUSSION	8
Thermal Combustion Properties and Level of Contamination	8
Flame Resistance and Flame Spread	13
Heat Release Rate Simulations of Contaminated Blankets	15
CONCLUSIONS	17
REFERENCES	18
APPENDICES	
A—Preliminary Report, Smoke Incident, Republic of China (Taiwan), February 23, 2008	
B—Material Analysis of Insulation Blanket From EVA 747-400	

LIST OF FIGURES

Figure		Page
1	Burned Thermal Acoustic Insulation in the February 23, 2008, Fire Event on EVA BR67	1
2	Thermal Acoustic Insulation Samples, Part Numbers, and Locations	3
3	Film Specimens Removed From the Inboard-Facing Thermal Acoustic Insulation Bags, Contamination Level, and Part Number	4
4	Specific Heat Release Rate Versus Temperature for Insulation Bagging Films in MCC	9
5	Heat Release Capacity of In-Service Insulation Blanket Encapsulating Films Versus the Weight Fraction of Contamination on the Specimen	10
6	Fire Load Versus Areal Weight of Contamination for In-Service Thermal Acoustic Insulation Blanket Encapsulating Films	11
7	Areal Heat Release Rate Versus Areal Weight of Contamination for In-Service Thermal Acoustic Insulation Blanket Encapsulating Films	12
8	Solid Residue of 2702 Film After Thermoxidative Degradation	13
9	Flame Spread Test Results at Different Ignition, Midway Through the Test, and at Flame Extinction for the 2702 Sample ($L = 4/5$), the 4606 Sample ($L = 3/4$), and the 2383 Sample ($L = 1$)	15
10	Heat Release Rate Versus Time Simulation for Insulation Blanket With a 3-mm-Thick (162 g/m^2) Surface Layer of Contamination	16
11	Heat Release Rate Versus Areal Weight of Contamination	17

LIST OF TABLES

Table		Page
1	Test Matrix for Thermal Acoustic Insulation Blankets and Films	2
2	Combustion Characteristics of Inboard-Side (Thick) Thermal Acoustic Insulation Blanket Encapsulating Films	8
3	Results of Flame Spread and Flame Resistance Tests of In-Service Thermal Acoustic Insulation Blankets and Films	14

LIST OF SYMBOLS AND ACRONYMS

λ	Specific heat of combustion of the specimen
η	Heat release capacity
μ	Pyrolysis residue
h	Specific heat of combustion of the specimen
h_g	Specific heat of combustion of the specimen gases
J/g	Joules per gram
L	Visual level of contamination
L_H	Visual level of horizontal contamination
L_V	Visual level of vertical contamination
Q	Specific heat release rate
W_A	Areal weight of film specimen
W_c	Areal weight of contamination
W_f	Areal weight of film
W/g	Watts per gram
CFR	Code of Federal Regulations
FAA	Federal Aviation Administration
HRR	Heat release rate
MCC	Microscale combustion calorimetry
PCFC	Pyrolysis-combustion flow calorimetry
PET	Polyethyleneterephthalate

EXECUTIVE SUMMARY

Thermal acoustic insulation blankets are widely used in commercial aircraft to provide thermal insulation and acoustic damping. This report examines the burning effects on the thermal acoustic insulation blankets retrieved from the EVA Airways Flight BR67 fire event. On February 23, 2008, passengers disembarking from EVA Airways Flight BR67 reported smoke in the cabin of the Boeing 747-400 after landing at Suvamabhumi International Airport in Bangkok, Thailand. An investigation of the incident revealed burned thermal acoustic insulation blankets. The level of contamination on the polyethyleneterephthalate film encapsulating the fiberglass insulation (blanket) was measured gravimetrically, ranked by visual inspection, and characterized by microscale combustion calorimetry to determine the thermal combustion properties and fire hazard. For the specimens tested, the areal weight of visible contamination was as high as 167 grams per square meter of film surface and its average heat of combustion was 13 kJ/g. Previous analysis by the aircraft manufacturer had determined that the contamination consisted of dried liquid corrosion-inhibiting compounds and particulate matter that included glass fibers, synthetic and natural fibers, animal hair, cotton fibers, mineral particles, plastic, Styrofoam, metal fragments, and insects. The present study determined that the inert/mineral component of the contamination accounted for about 1/3 of the weight of the contamination and was mostly broken glass fibers. The pyrolyzable (volatile) component accounted for the remaining 2/3 of the contamination and the specific heat of combustion of these volatile compounds ranged from 19-28 kJ/g. Insulation blankets and films were also tested for flame resistance and flame spread using regulatory and voluntary standards, respectively. All samples of insulation blankets passed the 12-second vertical Bunsen burner flame resistance requirement of Title 14 Code of Federal Regulations 25.853 and 25.855, but visibly contaminated blankets failed the nonregulatory (voluntary) screening test for flame spread using a cotton swab ignition source. Numerical modeling of the one-dimensional (through-thickness) burning rate suggests the flame-spread results may be associated with the nonuniform heat release rate of the contamination.

INTRODUCTION

Thermal acoustic insulation blankets are widely used in commercial aircraft to provide thermal insulation and acoustic damping. This report examines the burning effects on the thermal acoustic insulation blankets retrieved from the EVA Airways Flight BR67 fire event. On February 23, 2008, passengers disembarking from EVA Airways Flight BR67 reported smoke in the cabin of the Boeing 747-400 after landing at Suvamabhumi International Airport in Bangkok, Thailand. An investigation of the incident revealed burned thermal acoustic insulation blankets, as shown in figure 1. On May 6, 2008, the burned thermal acoustic insulation blankets that had visible contamination were carefully removed, rolled up, and covered with plastic film to preserve the level and location of the contamination (appendix A). The field inspection at the time reported the contamination to be dust, cotton fibers, and unknown hairs. The subsequent aircraft manufacturer's analyses of these blankets (appendix B) identified the plastic film encapsulating the fiberglass insulation as polyethyleneterephthalate (PET) and the surface contamination of the insulation bagging films as dried liquid corrosion-inhibiting compounds. The particulate matter was identified as glass fibers, synthetic and natural fibers, animal hair, cotton fibers, mineral particles, plastic, Styrofoam, metal fragments, and insects. In this study, the combustion characteristics of the in-service, thermal acoustic insulation blankets and encapsulating films were measured by microscale combustion calorimetry, and the flame resistance and flame spread performance were measured using standardized Federal Aviation Administration (FAA) tests.



Figure 1. Burned Thermal Acoustic Insulation in the February 23, 2008, Fire Event on EVA BR67

MATERIALS

In-service thermal acoustic blankets were obtained from the vicinity of the fire event on the Boeing 747-400. The thermal acoustic insulation blankets, designated by part numbers, consisted of a layer of low-density fiberglass insulation several centimeters thick that was entirely encapsulated by PET film. Thermal combustion properties were measured by microscale combustion calorimetry (MCC), and flame resistance and flame spread were measured for films and blankets (fiberglass batting encapsulated by film). The film facing the inside of the airplane was about 0.06 mm (0.002 inch) thick and is designated the inboard side in table 1. The film facing the fuselage was about 0.02 mm (0.0006 inch) thick and is designated the outboard side in table 1. The location of some of the samples is shown in figure 2.

Table 1. Test Matrix for Thermal Acoustic Insulation Blankets and Films

Part Number	Specimen	MCC	Flame Resistance	Flame Spread
411U4055-1037	Film	–	O	–
	Blanket	–	O	–
411U4120-2383	Film	–	O	–
	Blanket	–	O	I
411U4120-2386	Film	–	O	–
	Blanket	–	O	I
411U4120-2702	Film	I	I/O	–
	Blanket	–	I/O	I
411U4120-4302	Film	–	–	–
	Blanket	–	I/O	–
411U4120-4606	Film	I	I/O	–
	Blanket	–	I/O	I

I = Inboard face
O = Outboard face

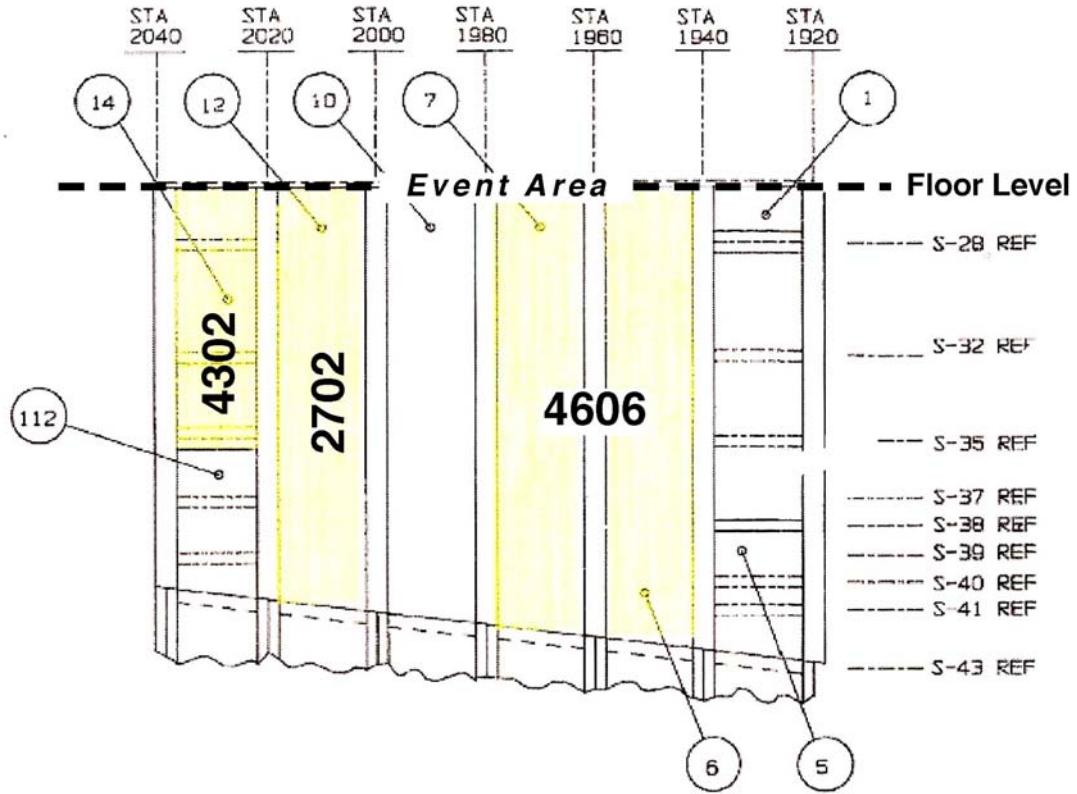


Figure 2. Thermal Acoustic Insulation Samples, Part Numbers, and Locations

METHODS

LEVEL OF CONTAMINATION BY VISUAL INSPECTION.

Thermal acoustic insulation blankets from EVA Airways Flight BR67 were removed from the aircraft and sent to the FAA William J. Hughes Technical Center, Atlantic City International Airport, New Jersey, for flammability tests. Thermal acoustic insulation blankets were also sent to the aircraft manufacturer for analysis of the contamination (see appendix B). Visual examination of the samples indicated that they were not contaminated uniformly over the surface. A qualitative ranking of the visible level of contamination of the 7-mm-diameter film specimens, ranging from 1 (no contamination) to 5 (highly contaminated), is shown in figure 3.

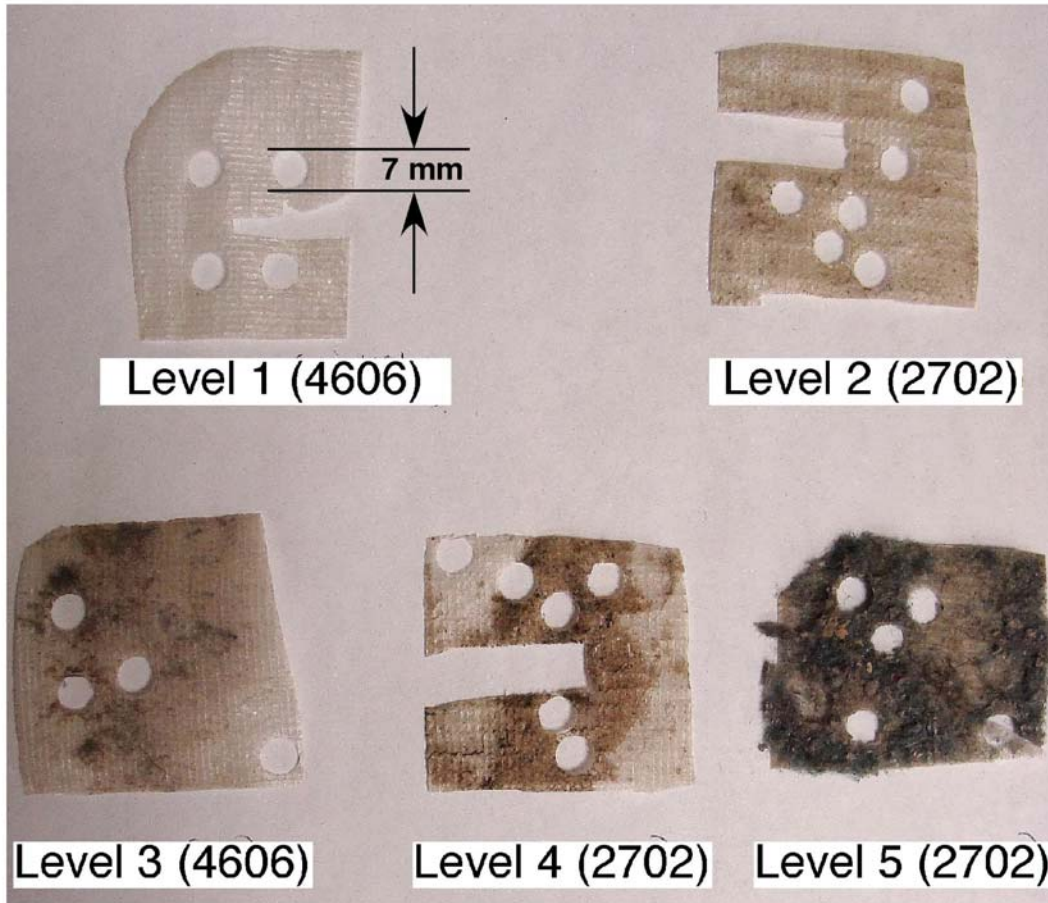


Figure 3. Film Specimens Removed From the Inboard-Facing Thermal Acoustic Insulation Bags, Contamination Level, and Part Number

GRAVIMETRIC DETERMINATION OF LEVEL OF CONTAMINATION.

Specimens for gravimetric determination of the level of contamination were obtained by cutting the inboard-facing encapsulating film of the 2702 and 4606 thermal acoustic insulation blankets using a circular punch with an inner diameter of 7 mm, as shown in figure 3. This produced a uniform 7-mm-diameter circular specimen with a surface area of $3.8485 \times 10^{-5} \text{ m}^2$. The circular specimens cut from the encapsulating films were weighed under ambient conditions without conditioning using an analytic balance with microgram resolution (Model C-31, CAHN). Samples ranged in mass from 0.7 mg for thin/outboard-side films to 9 mg for contaminated, thick/inboard-side films, depending on the level of contamination.

COMBUSTION PROPERTIES OF IN-SERVICE FILMS BY MICROSCALE COMBUSTION CALORIMETRY.

The same 7-mm-diameter circular specimens used to determine the level of contamination were analyzed in triplicate using MCC to determine their combustion characteristics. A standard method was used [1] in which the circular specimen was heated at a constant rate of temperature

rise $\beta = 1$ K/s from ambient temperature to 850°C. The pyrolysis gases generated during the heating program are purged from the sample chamber with nitrogen, mixed with excess oxygen, and combusted at 900°C for 10 seconds. The rate of heat released by combustion of the pyrolysis gases is calculated from the flow rate of the gas stream and the oxygen consumed. Four thermal combustion properties were measured during the typical 15-minute test.

SPECIFIC HEAT RELEASE RATE (Q). This is the time rate of evolution of combustion heat during the linear heating program at heating rate $\beta = 1$ K/s in units of Watts per gram of sample, W/g. The maximum value of the specific heat release rate is Q_{\max} .

HEAT RELEASE CAPACITY (η). This is the maximum rate at which combustion heat is released per degree of temperature rise during the heating program in units of J/g-K, i.e., the specific heat release rate normalized for heating rate.

$$\eta = \frac{Q_{\max}}{\beta}$$

PYROLYSIS RESIDUE (μ). This is the fraction of the original mass remaining at 850°C after pyrolysis in nitrogen during the MCC test in units of grams per gram of sample.

SPECIFIC HEAT OF COMBUSTION OF THE SPECIMEN (h). This is the integrated heat release rate (HRR), i.e., the area under the curve of heat release rate versus time, divided by the initial mass of specimen in units of Joules per gram of sample, J/g.

The following derived quantities are relevant to this report.

SPECIFIC HEAT OF COMBUSTION OF THE SPECIMEN GASES (h_g). This is the heat of combustion per unit mass of volatile pyrolysis products generated during the MCC heating program in units of Joules per gram of volatile mass, J/g.

$$h_g(J/g) = \frac{h}{1 - \mu}$$

AREAL WEIGHT OF FILM SPECIMEN (W_A). This is the combined areal weight of the film W_f and the contamination W_c per unit area of surface, g/m^2

$$W_A = \frac{\text{Specimen Mass}}{\text{Specimen Area}} = \frac{\text{Specimen Mass}}{3.849 \times 10^{-5} m^2} = W_f + W_c$$

AREAL WEIGHT OF FILM (W_f). This is the areal weight of the clean encapsulating film estimated from the average weight of the two specimens with the lowest mass (see results section)

$$W_f = \frac{(2.744 mg + 2.751 mg)/2}{3.849 \times 10^{-5} m^2} = 71.38 g/m^2$$

AREAL WEIGHT OF CONTAMINATION (W_c). This is the areal weight of the contamination on the encapsulating film, g/m^2

$$W_c = W_A - W_f$$

FIRE LOAD. This is the heat of combustion per unit area in units of J/m^2 calculated from the specific heat of combustion of the specimen h , and the specimen mass and area

$$Fire\ Load\ (J/m^2) = W_A h = (W_f + W_c) h$$

AREAL HEAT RELEASE RATE. The HRR is the rate at which combustion heat is released per unit area of film surface during the linear heating program in units of W/m^2 .

$$HRR\ (W/m^2) = Q_{max} W_A$$

FLAME RESISTANCE TEST FOR THERMAL ACOUSTIC INSULATION BLANKET.

Vertical Bunsen burner flame resistance tests were conducted on thermal acoustic insulation blankets and the encapsulating film as specified by Title 14 Code of Federal Regulations (CFR) Part 25 (Airworthiness Standards for Transport Category Aircraft), Sections 853 (Compartment Interiors) and 855 (Cargo or Baggage Compartments) according to recommended practices [2]. In these tests, a 75- x 305-mm specimen of insulation bag or the encapsulating film is cut from the blanket, clamped vertically in a draft-free cabinet, and subjected to a 38-mm Bunsen burner flame for 12 seconds. The 14 CFR 25.853 requirement for thermal acoustic insulation bags and films in the passenger cabin is that the average after-flame time of at least three specimens should not exceed 15 seconds; the average extinguishing time of flaming drips (if any) should not exceed 5 seconds; and the average burn length should not exceed 20 cm (8 inches).

THERMAL ACOUSTIC INSULATION BLANKETS FLAME SPREAD TESTS.

A nonregulatory cotton swab test for screening the flammability of thermal acoustic insulation blankets was conducted on entire insulation blankets according to a recommended procedure [3]. In the test, a thermal acoustic insulation blanket is forced against perpendicular, noncombustible surfaces to obtain an L-shape having a vertical surface that is 20.3 x 40.6 cm and a horizontal surface that is 40.6 cm square. To ignite the insulation blanket, the cotton tips are removed from the ends of a cotton swab, dipped in isopropyl alcohol, ignited, and placed at two locations: the intersection of the vertical and horizontal sections and in the center of the horizontal section. The guideline for flame spread of thermal acoustic insulation blankets is that no burn length shall exceed 20 cm (8 inches).

NUMERICAL MODELING OF BURNING RATE OF INSULATION BLANKETS.

The numerical pyrolysis model ThermaKin [4] was used to simulate the one-dimensional (through-thickness) burning rate of in-service aircraft thermal acoustic insulation blankets to determine the effect of uniform layers of contamination. The thermal acoustic insulation blanket was modeled as a system of three layers: surface contamination, encapsulating film, and

fiberglass insulation. Each layer was characterized by a set of thermal and physical properties, as described below.

SURFACE CONTAMINATION. The nominal composition of the as-received contamination was defined to be fiberglass wool (25% by weight) and volatile organic compounds (75% by weight), as per the gravimetric analysis. The density of the contamination was determined to be 54 kg/m^3 based on measurements of the weight, area, and thickness of the contamination that was removed from the thermal acoustic insulation blankets. The heat capacity of the contamination was set to 2000 J/kg-K [5], and the thermal conductivity was assumed to be temperature-dependent, with fiberglass having the major effect. The emissivity of the contamination was set equal to that of fiberglass, 0.94 [6], and the absorption coefficient was set to 1000, based on visual observation and the Lambert-Beer law. The surface contamination was assumed to thermally decompose via a first order reaction with Arrhenius activation energy $E_a = 47 \text{ kJ/mole}$ and frequency factor $A = 97 \text{ s}^{-1}$ obtained from pyrolysis-combustion flow calorimetry (PCFC) experiments. The heat of combustion of the volatile component was determined by PCFC to be 13.6 kJ/g . The heat of gasification was calculated from the volatile mass fraction and the heat of vaporization (360 J/g) of the hydrocarbon oils [5]. Simulations were also conducted in which the contamination was entirely composed of the C_{14} - C_{17} hydrocarbon oils having a density of 770 kg/m^3 , a constant thermal conductivity of 0.11 W/m-K , and an absorption coefficient (2000) [7] and emissivity (0.88) [8] that are typical of hydrocarbon polymers.

ENCAPSULATING FILM. The PET encapsulating film had a thickness of 50 micrometers (0.002 inch), a density of 1300 kg/m^3 , a thermal conductivity of 0.22 W/m-K [9], and a heat capacity that was temperature-dependent [10]. An absorption coefficient of 7000 was calculated [10] for PET, and a typical polymer emissivity of 0.88 [8] was used. The PET film was assumed to thermally decompose via a first order reaction with Arrhenius kinetic parameters $E_a = 110 \text{ kJ/mole}$, $A = 8.1 \times 10^{-5} \text{ s}^{-1}$. The heat of combustion of 24 kJ/g was determined by PCFC, and the heat of gasification (1800 J/g) was taken from reference 10.

FIBERGLASS INSULATION. The fibrous thermal acoustic insulation was modeled as a fiberglass blanket 2 cm thick with the same thermal and physical properties as the fiberglass component of the contamination layer, except that a density of 28 kg/m^3 was used, which is about half the density of the contamination layer. Increasing the thickness of the fiberglass wool insulation layer had no effect on the modeling results. A heat capacity of 1000 J/kg-K was used for the fiberglass insulation to include the effect of the binder.

Burning of the thermal acoustic insulation blanket was simulated in ThermaKin by exposing the contaminated surface to a constant radiant heat flux of 20 kW/m^2 to approximate the flame heat flux of the burning material. In the model, the one-dimensional system was divided into 20-micrometer-thick (0.0008-inch) elements, and the energy and mass conservation equations were solved for each element in 5-millisecond time steps. Reducing the thickness and time step by a factor of 5 to increase the accuracy of the integration did not significantly change the results of the simulations. ThermaKin burning rate simulations were conducted for thermal acoustic insulation blankets contaminated with the nominal composition of material (fiberglass/volatile organic compounds = 1/3, w/w) at thicknesses ranging from 0 to 15 mm in 1-mm increments.

ThermaKin burning rate simulations were also conducted for insulation blankets contaminated with only volatile organic compounds at thicknesses of 0, 0.03, 0.06, 0.12, 0.18, 0.3, 0.42, 0.5, and 0.6 mm. The HRR of the thermal acoustic insulation blanket in the ThermaKin simulation is the sum of the HRRs of the volatile contamination and insulation film, i.e., the sum of the products of the instantaneous pyrolysis rate ($\text{g/m}^2\text{-s}$) and the constant heat of combustion (J/g) of each component. Contamination thickness was converted to areal weight using the mass fractions and densities of the fiberglass and volatile organic components.

RESULTS AND DISCUSSION

THERMAL COMBUSTION PROPERTIES AND LEVEL OF CONTAMINATION.

Table 2 lists the results of the MCC tests, ranked in ascending order of specimen mass. A qualitative ranking of the visual level of contamination, L , of each specimen (see figure 3) is shown in table 2. The heat release capacity, η ; the specific heat of combustion of the specimen, h ; the residual mass fraction of the specimen after pyrolysis in the MCC test, μ , and the specific heat of combustion of the pyrolyzable (volatile) component, h_g , are given in table 2. All values in table 2 are the result of a single test at a heating rate $\beta = 1 \text{ K/s}$, so that Q_{\max} and η have the same numerical value but different units, i.e., W/g and J/g-K , respectively.

Table 2. Combustion Characteristics of Inboard-Side (Thick) Thermal Acoustic Insulation Blanket Encapsulating Films

Blanket	Specimen Mass (mg)	L	W_c (g/m^2)	η (J/g-K)	h (kJ/g)	μ (%)	h_g (kJ/g)
2702	2.744	1	$\equiv 0.00$	479	23.3	8.7	25.5
2702	2.751	1	$\equiv 0.00$	447	22.1	10.0	24.6
4606	2.821	1	1.91	470	24.7	6.4	26.4
2702	2.838	1	2.35	480	24.1	7.9	26.2
4606	2.915	2	4.35	525	26.2	5.8	27.8
4606	2.958	2	5.47	490	25.6	5.3	27.0
4606	2.987	2	6.23	468	26.2	5.0	27.6
4606	2.987	2	6.23	517	26.8	4.5	28.1
4606	2.998	2	6.51	516	26.1	5.5	27.6
4606	3.010	2	6.82	504	26.4	5.2	27.8
4606	3.055	2	7.99	523	25.7	6.2	27.4
2702	3.210	3	12.03	421	21.1	11.7	23.9
2702	3.257	3	13.25	455	23.5	8.6	25.7
4606	3.472	3	18.84	337	19.8	14.2	23.1
4606	3.525	3	20.22	402	22.3	10.5	24.9
2702	3.552	3	20.92	351	18.2	15.0	21.4

Table 2. Combustion Characteristics of Inboard-Side (Thick) Thermal Acoustic Insulation Blanket Encapsulating Films (Continued)

Blanket	Specimen Mass (mg)	L	W_c (g/m ²)	η (J/g-K)	h (kJ/g)	μ (%)	h_g (kJ/g)
2702	3.591	3	21.93	369	18.4	14.3	21.5
2702	4.058	3	34.08	341	20.2	13.6	23.4
2702	4.096	3	35.07	207	18.0	15.5	21.3
4606	4.445	3	44.14	320	17.9	17.3	21.6
2702	4.791	4	53.14	273	16.2	18.6	19.9
2702	5.024	4	59.20	251	15.8	19.1	19.5
2702	7.403	5	121.08	186	16.0	19.2	19.8
2702	7.814	5	131.76	218	15.4	19.2	19.1
2702	9.167	5	166.95	143	15.1	22.2	19.4

L = Contamination

Figure 4 contains representative experimental data for specific heat release rate Q (W/g) versus temperature for the samples in table 2. Figure 4 shows that the peak height, Q_{max} , and the total heat released by combustion of the pyrolyzate, h , (peak area) decrease with increasing level of contamination.

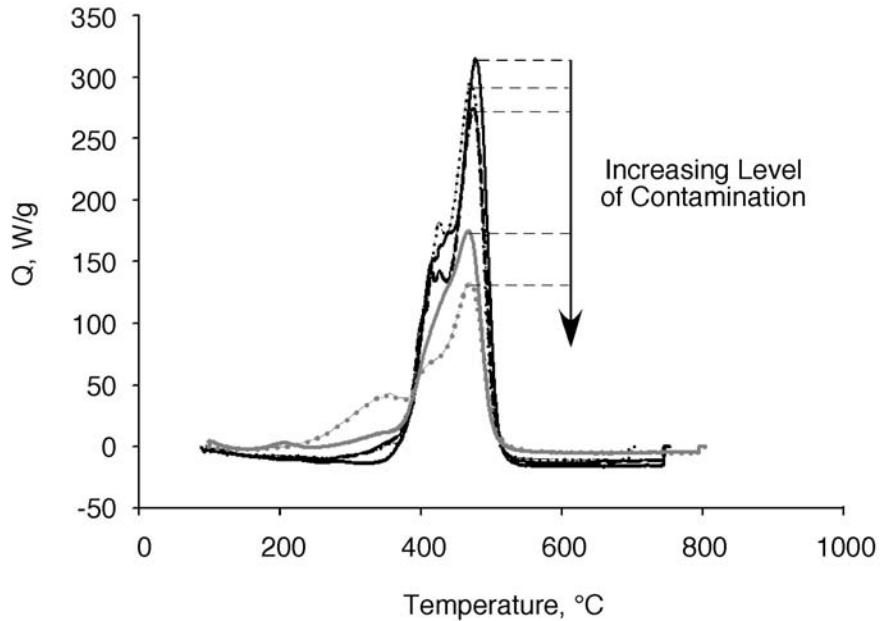


Figure 4. Specific Heat Release Rate Versus Temperature for Insulation Bagging Films in MCC

The heat release capacity of multicomponent materials, like most material properties, follows an upper-bound rule of mixtures with an interaction term [11]. For a two-component material, e.g., clean encapsulating film (f) and contamination (c), having heat release capacities and mass fractions η_f, w_f and η_c, w_c , respectively, the rule-of-mixtures for η takes the form:

$$\eta = w_f \eta_f + w_c \eta_c + \lambda(w_f w_c)^{1/2}(\eta_f + \eta_c) \quad (1)$$

The sign of the parameter λ in equation 1 determines whether the interaction between the two components produces a positive or negative deviation from ideal ($\lambda = 0$) behavior. In terms of the areal weights of the film W_f and contamination, W_c and their specific heat release rate maxima, $Q_f = \beta\eta_f$ and $Q_c = \beta\eta_c$, equation 1 becomes

$$Q_{\max} = \beta \eta = \frac{W_f Q_f + W_c Q_c + \lambda(W_f W_c)^{1/2}(Q_f + Q_c)}{W_f + W_c} \quad (2)$$

Equation 2 was fit to the HRR data in table 2 using a weighted, nonlinear least squares regression. For the film areal weight of table 2, $W_f = 71.4 \text{ g/m}^2$, the best-fit values of the three remaining adjustable parameters were $Q_f = 532 \text{ J/g-K}$, $Q_c = 110 \text{ J/g-K}$, and $\lambda = -0.28$, with a correlation coefficient of $R = 0.94$. These parameters were used in equation 2 to generate the solid line in figure 5. The dashed line in figure 5 was generated with these same parameters, assuming a simple rule of mixtures ($\lambda = 0$). Figure 5 demonstrates that a negative interaction between the film and contamination best captures the MCC data. The negative interaction parameter probably reflects the fact that the contamination releases combustion heat over a broader temperature range than does the PET film (see figure 4) in the MCC.

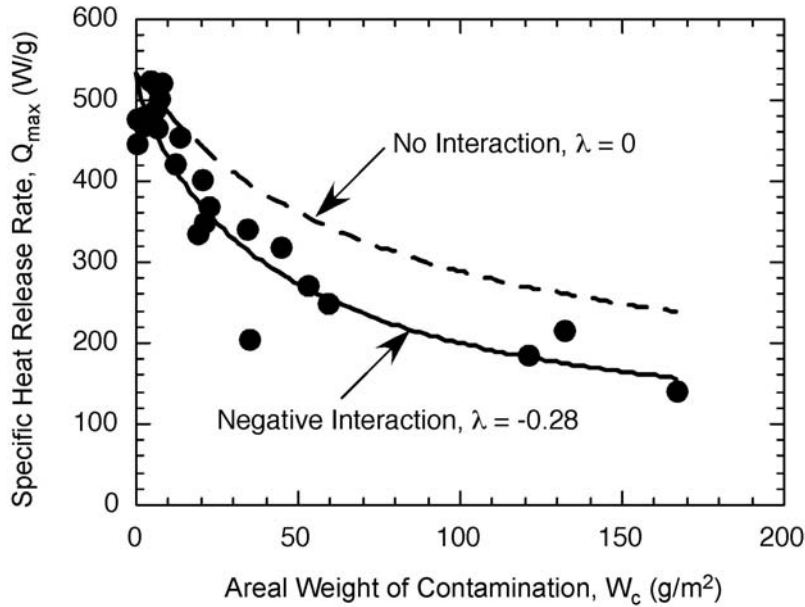


Figure 5. Heat Release Capacity of In-Service Insulation Blanket Encapsulating Films Versus the Weight Fraction of Contamination on the Specimen

The specific heat of combustion of the contamination, $h_c = (h \times \text{Specimen Mass})/(\text{Mass of Contamination})$ is very sensitive to low levels of contamination, yielding unreasonably high values at low levels. An average value that is strongly weighted for the level of contamination, is

$$\bar{h}_c = \frac{\sum W_{c,i}^2 h_{c,i}}{\sum W_{c,i}^2} = 13 \text{ kJ/g}$$

This is roughly half the heat of combustion of the clean PET film, $h_f = 23 \text{ kJ/g}$ (the first two values of h in table 2). Figure 6 is a plot of the heat of combustion per unit area of encapsulating film (fire load) versus the areal mass of contamination. The solid circles are $h \text{ (J/g)} \times W_A \text{ (g/m}^2\text{)}$ in table 2. The solid line is calculated from the simple rule of mixtures,

$$\text{Fire Load} = h_f W_f + h_c W_c = 1600 \frac{\text{J}}{\text{m}^2} + 13 \frac{\text{kJ}}{\text{g}} W_c \quad (3)$$

Equation 3 captures the trend of the experimental values in figure 6 reasonably well with no adjustable parameters.

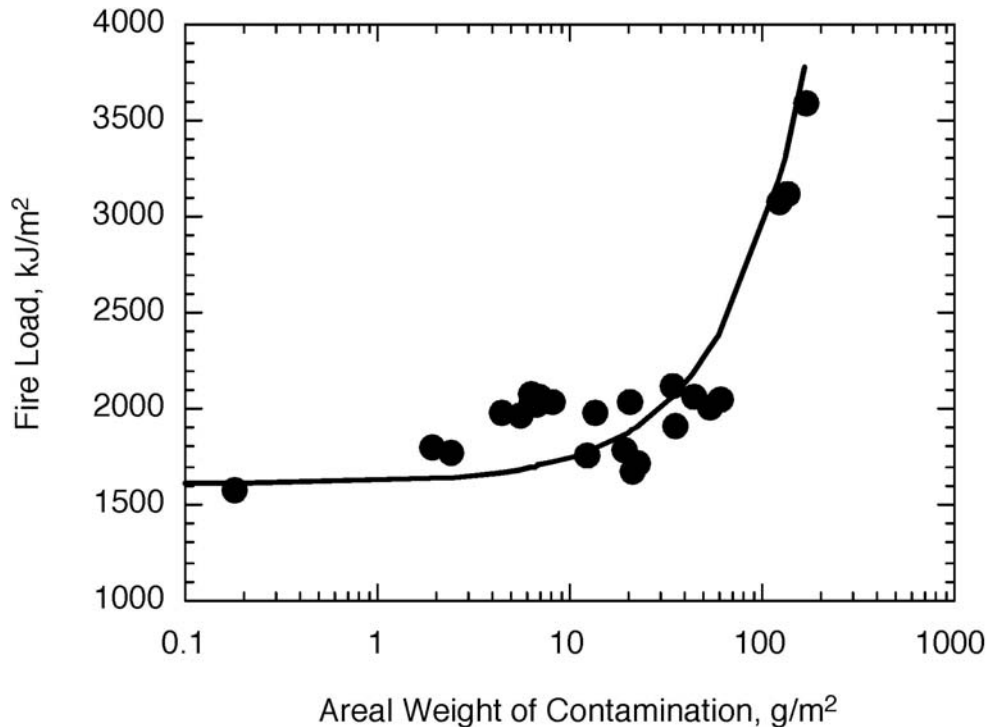


Figure 6. Fire Load Versus Areal Weight of Contamination for In-Service Thermal Acoustic Insulation Blanket Encapsulating Films

Heat release rate is known to be a primary indicator of the fire hazard potential of a material in an aircraft cabin [12]. Figure 7 shows a plot of the areal heat release rate, $\text{HRR (W/m}^2\text{)} = Q_{\text{max}} \times W_A$ versus the areal weight of contamination W_c on the thermal acoustic insulation encapsulating

films calculated from the data in table 2. Figure 7 shows that the HRR of the in-service encapsulating film is independent of the level of contamination, i.e., contamination does not significantly increase the HRR of insulation blankets as measured in the MCC. This result is a consequence of the negative interaction between the film and contamination. According to equation 2, the HRR can be rewritten in terms of the areal weights of the film W_f and contamination W_c and their peak heat release rates, $Q_f = 532 \text{ W/g}$ and $Q_c = 110 \text{ W/g}$

$$\begin{aligned}
 HRR &= W_A Q_{\max} = W_f Q_f + \{W_c Q_c + \lambda(W_f W_c)^{1/2}(Q_f + Q_c)\} \\
 &= 38 \text{ kW/m}^2 + \{W_c Q_c - 0.28(W_c W_f)^{1/2}(Q_f + Q_c)\} \\
 &\approx 38 \text{ kW/m}^2 - 3 \pm 2 \text{ kW/m}^2 = 35 \pm 2 \text{ kW/m}^2
 \end{aligned}
 \tag{4}$$

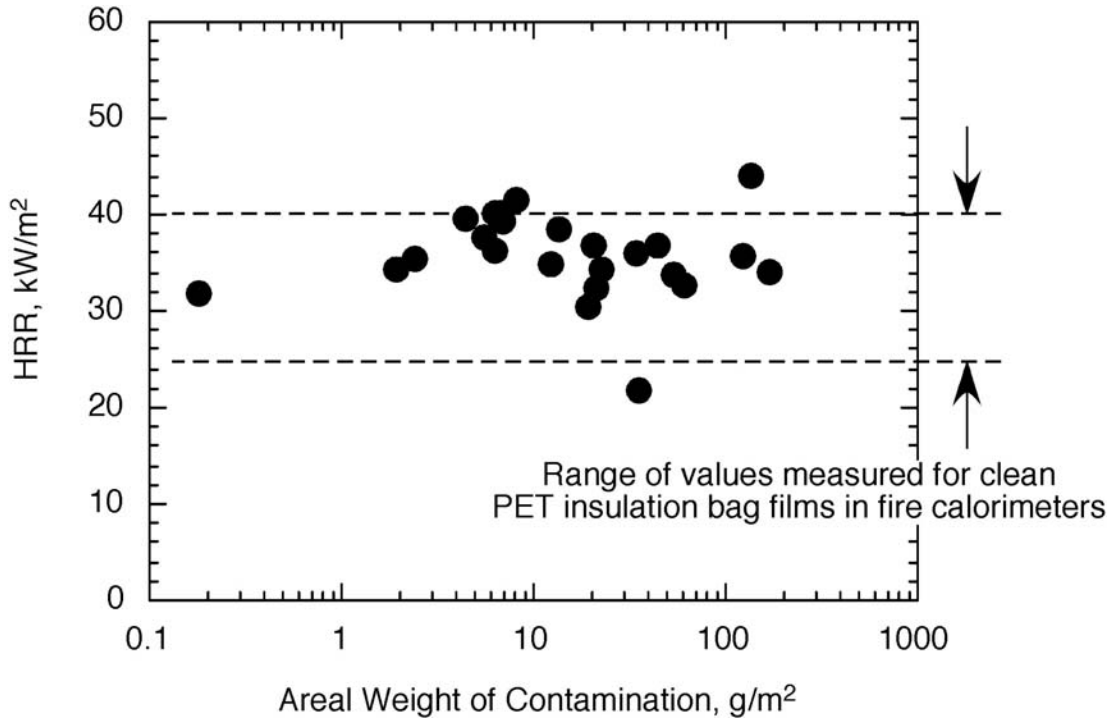


Figure 7. Areal Heat Release Rate Versus Areal Weight of Contamination for In-Service Thermal Acoustic Insulation Blanket Encapsulating Films

Thus, the HRR plotted in figure 7 is independent of the level of contamination because the interaction (bracketed) term in equation 4 has a small, relatively constant, negative value ($-3 \pm 2 \text{ kW/m}^2$, two standard deviations) that offsets the fire load of the contamination. The insensitivity of HRR to W_c in the MCC may be a consequence of the idealized chemical nature of the test, in which the specimen is subjected to forced, nonflaming, complete combustion, and physical effects, such as melting, shrinking, and flame spread, are not accounted for. However, the HRR of the in-service insulation films measured in the MCC are in the same range (dashed lines in figure 7) as the HRR of clean PET insulation films measured in flaming combustion in a fire calorimeter at external heat fluxes from ranging from 20 to 75 kw/m^2 [13].

Figure 8 shows a 40X optical photograph of the solid residue remaining after thermoxidative degradation (1 hour in air at 650°C) of the contamination removed from a 2702 film. The photograph shows that the residue that remains after the organic matter is oxidized is primarily glass fibers.

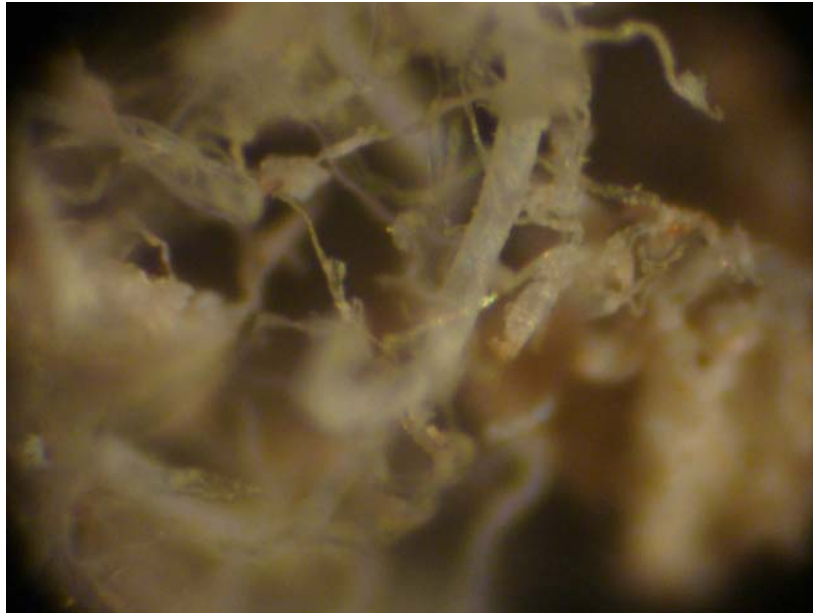


Figure 8. Solid Residue of 2702 Film After Thermoxidative Degradation

FLAME RESISTANCE AND FLAME SPREAD.

Table 3 contains the results of single-flame spread tests and the average results of 1-3 flame resistance tests conducted on the thermal acoustic insulation blankets and encapsulating films. The first column is the part number from which the specimen in the second column was taken. The visible level of contamination $L = 1-5$ (see figure 3) is estimated in the second column for the flame spread test specimens (blankets). The third and fourth columns are the horizontal (L_H) and vertical (L_V) flame spread lengths in the alcohol-soaked cotton swab ignition test of blankets. The fifth column designates the Inboard (0.06-mm-thick) or Outboard (0.02-mm-thick) film face, F , tested for flame resistance, while columns 6-8 contain the time of flaming, t_f , after removal of the Bunsen burner flame, the burn length, L_b , and the after-flame time of burning drips, t_{fd} , respectively. It is shown that all of the inboard and outboard in-service films and blankets passed the requirements for 14 CFR 25.853 flame resistance, regardless of the level of contamination. Conversely, only blankets with little ($L = 1$ to $2 = 1/2$) or no ($L = 1$) visible contamination passed the cotton swab screening test for flame spread. Figure 9 contains photographs of the cotton swab test results for the 2383, 2702, and 4606 blankets at ignition (2602), at flame extinction (2383, 2702, and 4606), and midway through the test (2702 and 4606). Figure 9 shows that the extent of flame spread for the contaminated blankets 2702 and 4606 far exceeds that for the uncontaminated blankets 2383 and 2386 (not shown). The greater flame spread of contaminated blankets may be the result of chemical and physical effects. Chemical effects are associated with the increased fire load of the contamination and its ease of ignition as a low-density fuel source. Physical effects include the mechanical constraint imposed

on the encapsulating film by the fibrous contamination that prevents the film from shrinking away from the ignition source (flame) and acts as a substrate for wicking of molten/flaming droplets.

Table 3. Results of Flame Spread and Flame Resistance Tests of In-Service Thermal Acoustic Insulation Blankets and Films

Part Number	Specimen Form	Flame Spread			Flame Resistance		
		L _H	L _V	F	t _F	L _b	t _{fd}
		cm	cm		sec	cm	sec
411U4055-1037	Film	–	–	O	0	<2.5	0
	Blanket	–	–	O	0	8	0
411U4120-2383	Film	–	–	O	0	<2.5	0
	Blanket			O	0	11.6	0
	Blanket (L = 1)	8	13	I			
411U4120-2386	Film	–	–	O	0	<2.5	0
	Blanket			O	0	11.6	0
	Blanket (L = 1/2)	18	15	I			
411U4120-2702	Film	–	–	O	0	<2.5	0
	Film	–	–	I	0	<2.5	0
	Blanket	–	–	O	<1	8.9	0
	Blanket (L = 4/5)	20	41	I	11	8.9	0
411U4120-4302	Film	–	–	–	–	–	–
	Blanket	–	–	O	0	7.6	0
	Blanket	–	–	I	0	5	<1
411U4120-4606	Film	–	–	O	0	<2.5	0
	Film	–	–	I	0	2.5	0
	Blanket	–	–	O	0	8	0
	Blanket (L = 3/4)	23	30	I	0	8	0
REQUIREMENT		<20	<20		<15	<20	<5

F = Film face
 I = Inboard
 L = Visible level of contamination
 L_b = Burn length
 O = Outboard
 t_F = Time of flaming
 t_{fd} = After-flame time of burning drips

Note: A dash (–) means that no test was performed for this specimen.



Figure 9. Flame Spread Test Results at Different Ignition, Midway Through the Test, and at Flame Extinction for the 2702 Sample ($L = 4/5$), the 4606 Sample ($L = 3/4$), and the 2383 Sample ($L = 1$)

HEAT RELEASE RATE SIMULATIONS OF CONTAMINATED BLANKETS.

Figure 10 shows the HRR history of an insulation blanket with a 3-mm-thick (162 g/m^2) layer of the nominal contamination, as well as the separate HRRs of the film and contamination. Note the delay in the maximum HRR of the film relative to the contamination due to the insulating value of the latter.

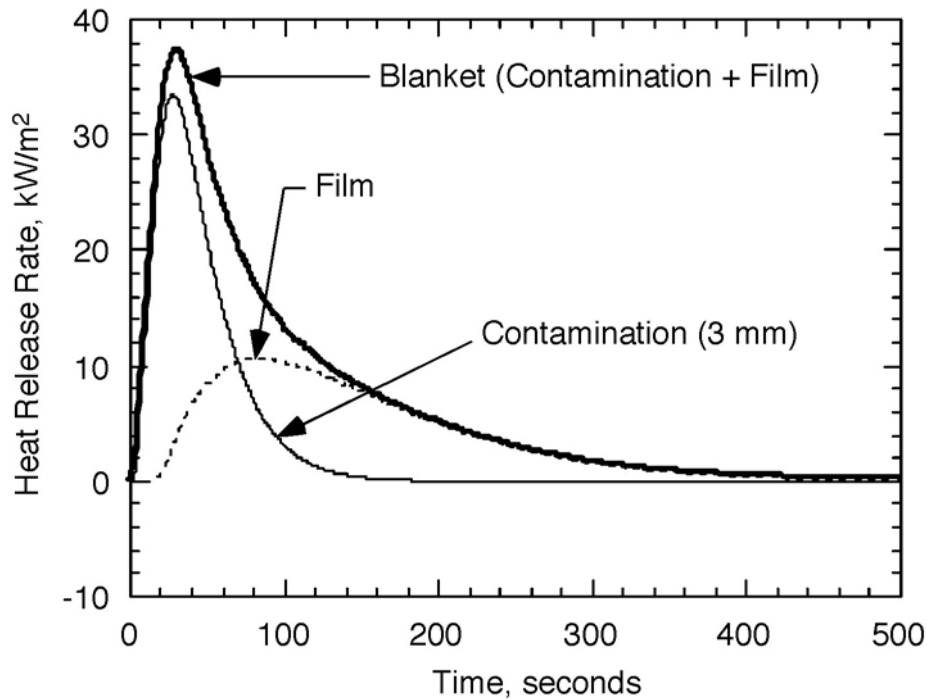


Figure 10. Heat Release Rate Versus Time Simulation for Insulation Blanket With a 3-mm-Thick (162 g/m^2) Surface Layer of Contamination

Figure 11 shows the ThermaKin simulation results for the maximum (peak) HRR of the insulation blanket versus the areal weight of contamination for the nominal composition (fiberglass + volatile organics) as a solid line. The dashed line in figure 11 represents the simulation results for the peak HRR of contamination that is entirely composed of volatile organics having the same heat of combustion as the volatile component of the nominal composition. It is clear that the peak HRR of the volatile organic contamination increases monotonically with areal weight because the contamination and PET film have similar thermal properties and therefore have synchronized (additive) burning rates. In contrast, the peak HRR of blankets contaminated with the nominal low-density composition (fiberglass/volatile organic = 1/3) reaches a broad maximum in the vicinity of 250 g/m^2 (5 mm thickness). This HRR plateau of contaminated blankets reflects steady burning of the low-density, thermally thick, predominantly fiberglass contamination. A maximum in the peak HRR is observed because, at high areal weight, the contamination acts as a thermal barrier that delays the burning of the underlying PET film so that their HRRs are no longer synchronized in time (see figure 10). The HRR simulations with no adjustable parameters are in the range of the HRRs calculated from MCC data and those measured in fire calorimeters (figure 7).

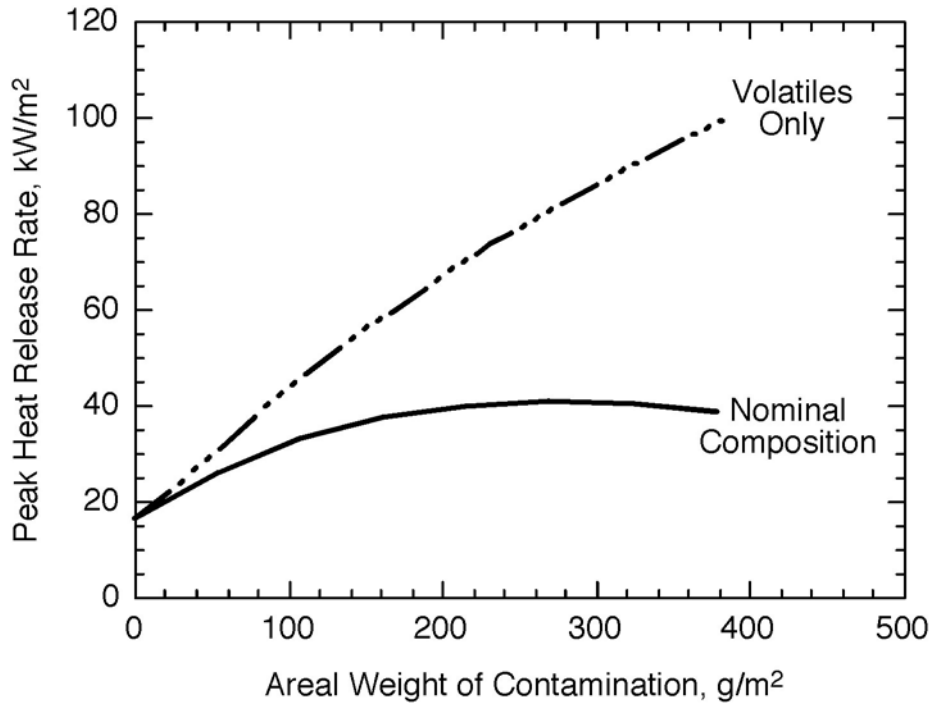


Figure 11. Heat Release Rate Versus Areal Weight of Contamination (Solid line is contamination that has the nominal composition. Dashed line is contamination that is completely volatile.)

The data in figure 11 suggest that the highly contaminated thermal acoustic insulation blankets pass the requirement for vertical flame resistance but fail the voluntary flame spread guidelines of the cotton swab test. Shrinkage of contaminated insulation films from the heat of the Bunsen burner is a physical mechanism that effectively removes the flammable material from the ignition source in the two-dimensional vertical flame resistance test. Film shrinkage away from the ignition source is precluded in the three-dimensional flame-spread test because the ignition source (surface flame) travels with the shrinking film in both the horizontal and vertical directions (see figure 9). Assuming a critical heat release for flame spread of 50-60 kW/m² [14] in the cotton swab test, figure 11 shows that nonuniform contamination at levels above 150 g/m² could lead to variable two-dimensional burning as the flame spreads across regions of volatile (high HRR) contamination, as shown in figure 9.

CONCLUSIONS

The following conclusions regarding the flammability of contaminated in-service thermal acoustic insulation blankets follow directly from the Results and Discussion.

- The areal weight of contamination was as high as 167 g/m² in this study.
- The heat of combustion of the contamination ranged from 5 to 28 kJ/g, with an average of 13 kJ/g.

- The fire load (J/m^2) increases with the areal weight of contamination because of its finite heat of combustion. The fire load triples at the highest level of contamination.
- Inert material (glass fibers, mineral particles, and metal fragments) comprised about one-third of the weight of the contamination.
- Volatile materials (polyethyleneterephthalate film, corrosion inhibiting compounds, synthetic and natural fibers, animal hair, cotton fibers, plastic, Styrofoam, and insects) comprised about two-thirds of the weight of the contamination and its heat of combustion ranged from 19 to 28 kJ/g, with an average value of 24 kJ/g.
- All contaminated samples passed the regulatory requirement for flame resistance of thermal acoustic insulation in passenger and cargo compartments using a vertical Bunsen burner test with a 12-second ignition according to Title 14 Code of Federal Regulations 25.853 and 25.855.
- Visibly contaminated thermal acoustic insulation failed the voluntary screening test for flame spread using an alcohol-soaked cotton swab ignition source.
- Failure of the voluntary flame spread guideline for in-service thermal acoustic insulation blankets at measured levels of contamination may be due to the different heat release rates of various types of contamination.

REFERENCES

1. “Standard Test Method for Determining Flammability Characteristics of Plastics and Other Solid Materials Using Microscale Combustion Calorimetry,” ASTM D 7309-07, American Society for Testing and Materials (International), West Conshohocken, Pennsylvania, 2007.
2. Horner, A., ed., “Aircraft Materials Fire Test Handbook,” Chapter 1: Vertical Bunsen Burner Test for Cabin and Cargo Compartment Materials, FAA report DOT/FAA/AR-00/12, April 2000.
3. Horner, A., ed., “Aircraft Materials Fire Test Handbook,” Chapter 22: Cotton Swab Test for Thermal Acoustic Insulation Blankets, FAA report DOT/FAA/AR-00/12, April 2000.
4. Stoliarov, S.I. and Lyon, R.E., “Thermo-Kinetic Model of Burning,” FAA report DOT/FAA/AR-TN08/17, May 2008.
5. Weast, R.C. and Astle, M.J., eds., *Handbook of Chemistry and Physics*, 63rd ed., CRC Press, Inc., Boca Raton, Florida, 1982.
6. Holman, J.P., *Heat Transfer*, McGraw Hill, New York, New York, 1997.

7. Tsilingiris, P.T., "Comparative Evaluation of the Infrared Transmission of Polymer Films," *Energy Conversion and Management*, Vol. 44, 2003, pp. 2839-2856.
8. Hallman, J.R., "Ignition Characteristics of Plastics and Rubber," Ph.D. Thesis, the University of Oklahoma, 1971.
9. Lyon, R.E., "Plastics and Rubber" *Handbook of Building Materials for Fire Protection*, Harper, C.A., ed., McGraw-Hill, New York, New York, 2004.
10. Stoliarov, S.I. and Walters, R.N., "Determination of the Heats of Gasification of Polymers Using Differential Scanning Calorimetry," *Polymer Degradation and Stability*, Vol. 93, 2008, pp. 422-427.
11. Lyon, R.E. and Emrick, T., "Non-Halogen Fire Resistant Plastics for Aircraft Interiors," *Polymers for Advanced Technologies*, Vol. 19, 2008, pp. 609-619.
12. Sarkos, C.P., "An Overview of Twenty Years of R&D to Improve Aircraft Fire Safety and Security," *Fire Protection Engineering*, Vol. 5, 2000, pp. 4-16.
13. Gandhi, S., Quintiere, J.G., and Lyon, R.E., "Flammability of Aircraft Thermal Insulation Films," *45th International SAMPE Symposium*, Long Beach, California, May 21-25, 2000.
14. Lyon, R.E. and Quintiere, J.G., "Piloted Ignition of Combustible Solids," *Combustion & Flame*, Vol. 151, 2007, pp. 551-559.

APPENDIX A—PRELIMINARY REPORT, SMOKE INCIDENT, REPUBLIC OF CHINA
(TAIWAN), FEBRUARY 23, 2008

The Preliminary Report, Smoke Incident, Republic of China (Taiwan), February 23, 2008, is attached. (In the Navigation Pane on the left, click on the "paper clip" to access the attached file.)

APPENDIX B—MATERIAL ANALYSIS OF INSULATION BLANKET FROM EVA 747-400

BACKGROUND:

A fire incident was reported in an EVA 747-400 cargo bay. The insulation blankets from the fire area and near that area were removed. The Flammability, Safety & Airworthiness and Standards Group of M&PT required more information as to the identity of contaminants found on the blankets' surfaces. Sections of insulation blankets involved in the incident and those near by were analyzed to characterize the contamination. The samples were labeled as follows:

1A; 2A; 2B; 3A; 3B; 3C; 3D; 5A;
6A; 6B; 6C; 7A; 7B; 7C

FTIR spectroscopy, EMPA, and PLM were used to identify contaminants and characterize the insulation blanket film. The samples can be seen in Figure 2.

SAMPLE DESCRIPTIONS:

The samples were surface pieces of insulation blanket film. Some samples were heavily contaminated with dust, dirt, fibers, and particulate matter. Also contamination included dried liquids. The samples as received with sampling areas identified can be seen in Figure 2.

RESULTS**Film Characterization:**

The exterior surface of the provided blanket film samples were analyzed to confirm the film was Polyethylene Terephthalate (PET) and determine contaminants present. Small sections of the film samples were rinsed with acetone to clean them (where no visible contamination was present). A scalpel was used to cut small pieces of the film out to sample with FTIR. The thermal analysis samples were sized about 1"x1". The blanket film samples were found to be consistent with PET as indicated by presence of characteristic peaks seen in Figure 1 below.

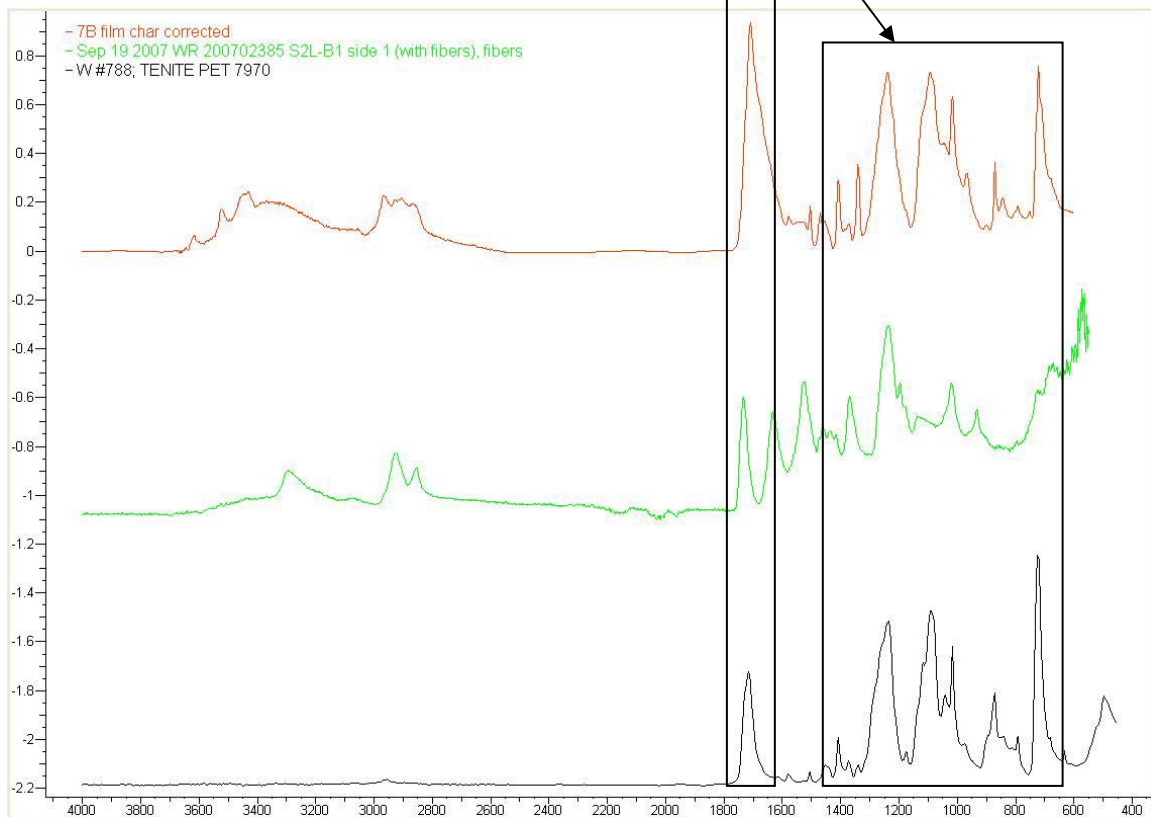






Figure 1: typical spectra of PET (black) compared to spectra of WR200702385 (green) a study of similar insulation blankets and a typical spectra of blanket film from sample 7B (red) showing blanket material is consistent with PET

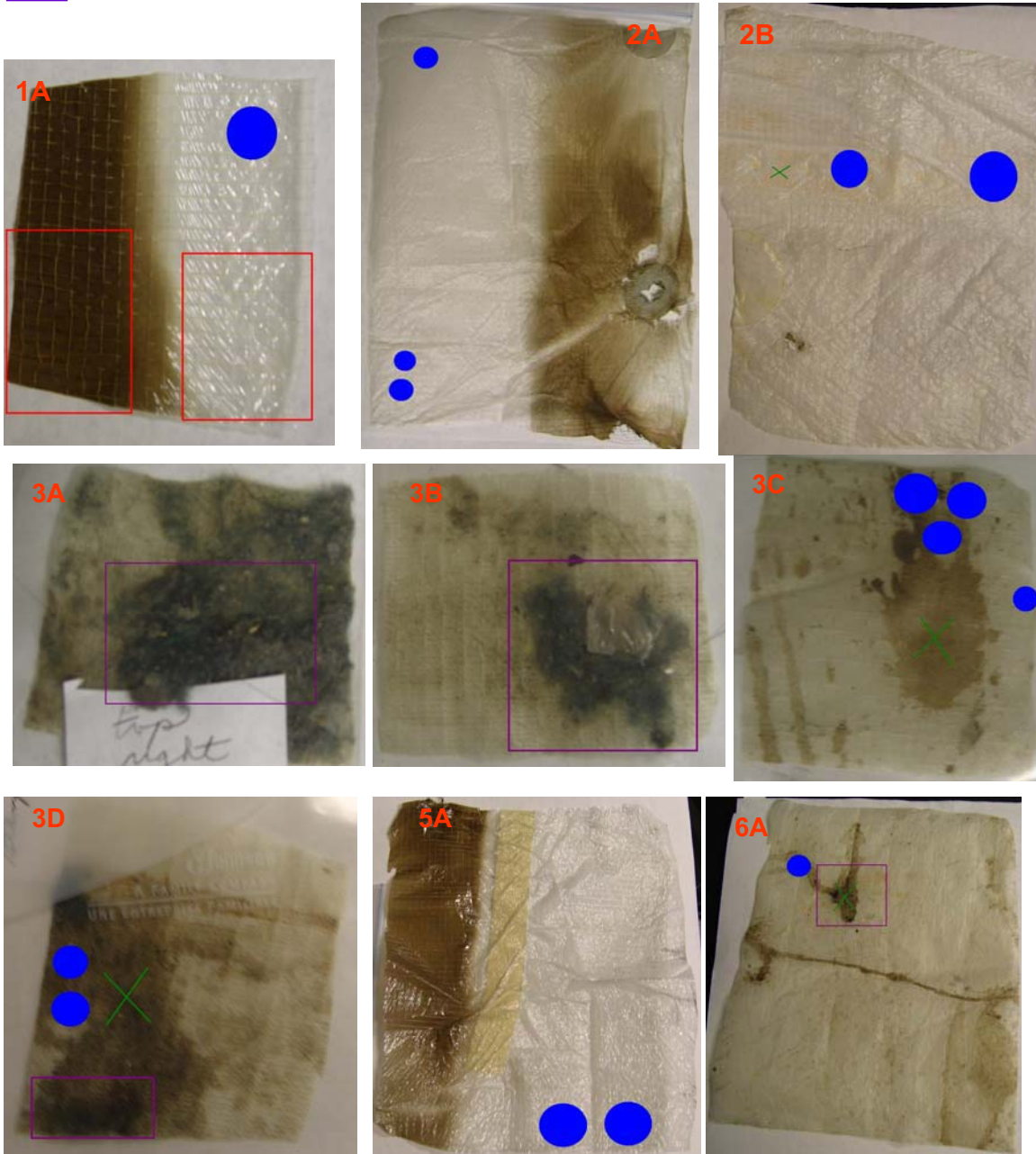
Surface Contamination Identification:

Sampling areas and techniques can be seen labeled below in Figure 2 and 2A. On sections of brown contamination the blanket films were rinsed with hexane/ acetone. The solvent was collected and allowed to evaporate. The resulting residue was analyzed with FTIR spectroscopy. In addition, flakes of the dried brown contaminate were removed. The FTIR spectra from both forms of sampling indicated the brown contamination was consistent with corrosion inhibiting compounds as seen in Figures 3 and 4. In addition, EMPA spectra from brown flakes were used, but samples proved to be heavily contaminated by surroundings, a representative spectrum can be seen in Figure 5 and a typical CIC spectrum is shown in Figure 6. Similarities can be seen but are hindered by the amount of contamination.

Figure 2: Films 1-7 Areas of Analysis

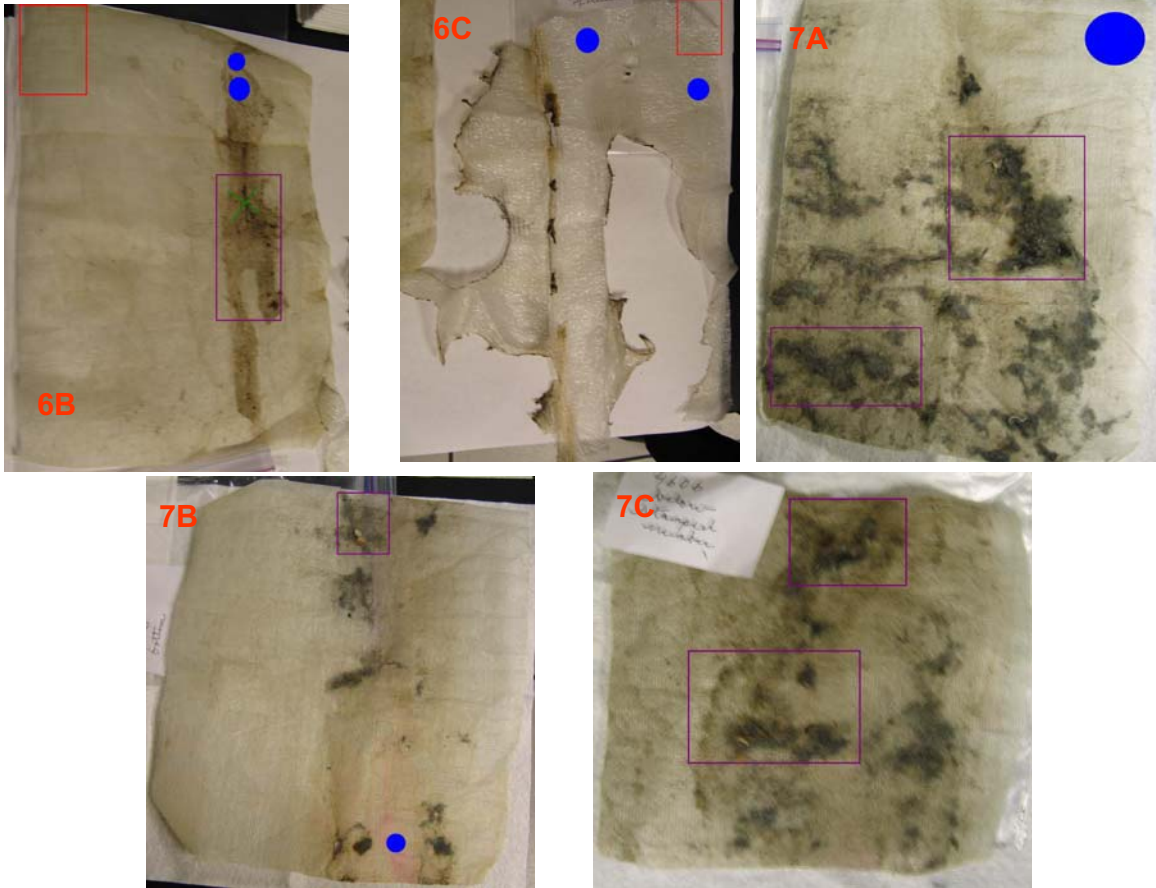
-  = Thermal analysis TGA
-  = FTIR analysis
-  = Microprobe sample
-  = particulate matter sampled

Part numbers listed in Table I



Note: no sample 4

Figure: 2A



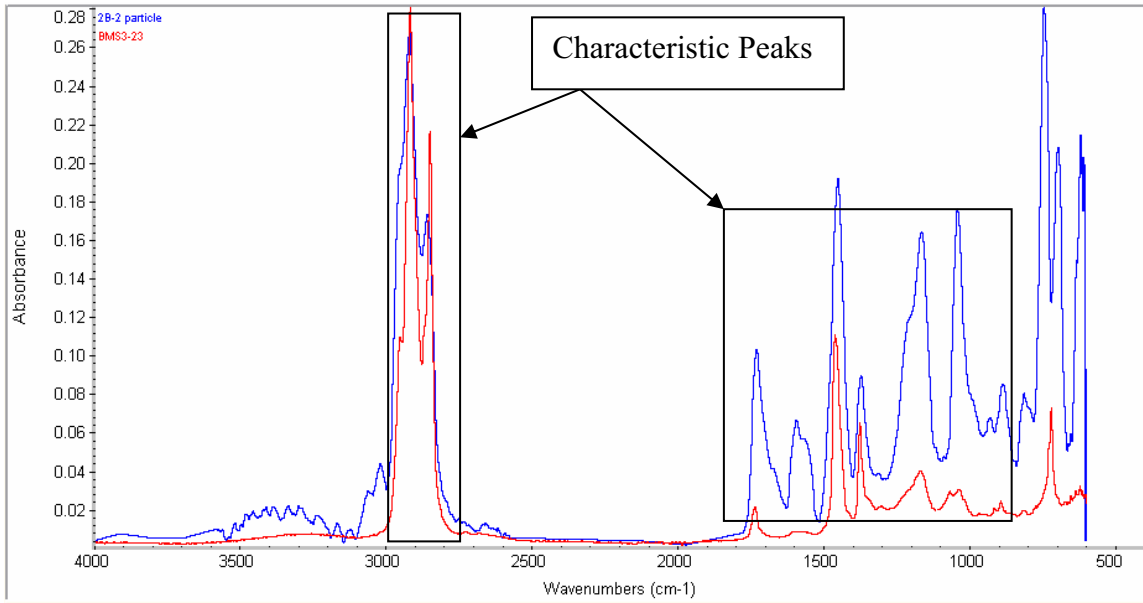


Figure 3: Flake removed from blanket 2B compared to BMS3-23, typical CIC spectra showing flake is consistent with CIC

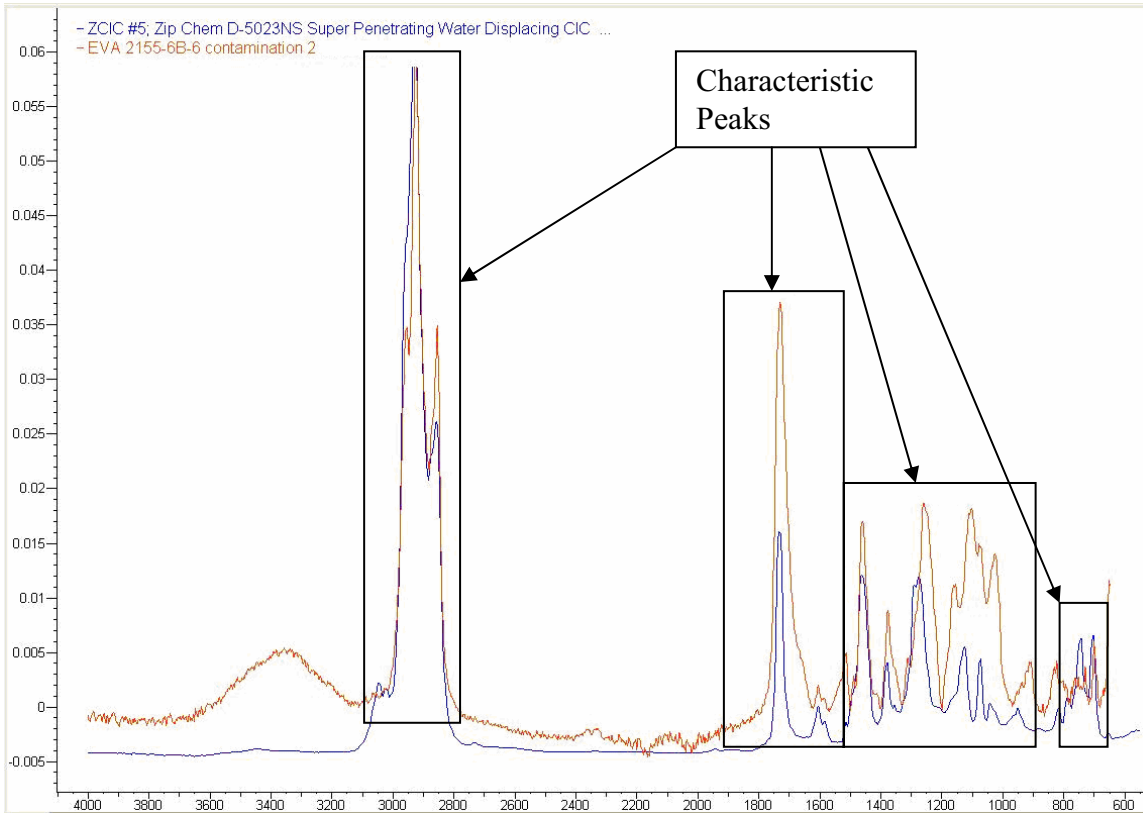


Figure 4: flake sample from blanket 6B compared to typical CIC spectra showing flake is consistent with CIC

C:\EDS Spectra\MimiLaberta\MLB 7.spc

Label A: MLB_7

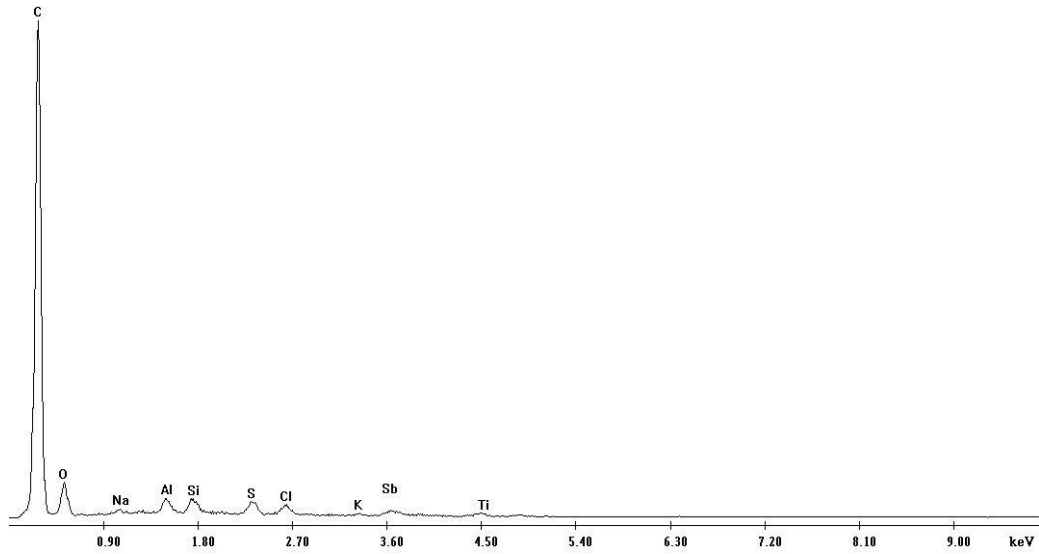


Figure 5: Representative EMPA sample of CIC flake removed from blanket surface

C:\EDS Spectra\wr8-2372\16173.spc

Label A: 16173

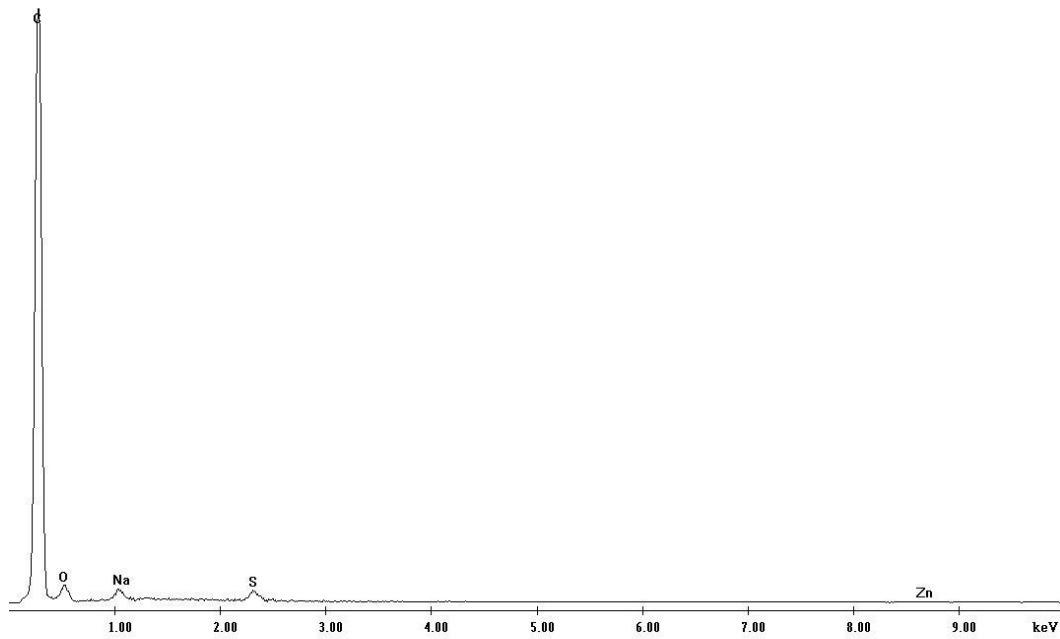


Figure 6: Typical CIC EMPA spectrum

Summary of Results: Table I

Surface Contamination on Insulation Film					
Part #	Blanket	Sample	Summary of Results	Thermal Analysis	Microprobe
411U4055-1037	1	1A	film id'ed as PET and areas of thermally damaged PET	√	
		1B	thermally damaged PET		
411U4120-2386	2	2A	film id'ed as PET		
		2B	contamination similar to CIC		√
411U4120-2702	3	3A	see Table II		
		3B	see Table II		
		3C	film id'ed as PET, contamination similar to CIC		√
		3D	contamination similar to CIC, possible hydraulic fluid		√
61B50025-1002	4		No sample received for this number		
411U4120-2383	5	5A	film id'ed as PET		
411U4120-4302	6	6A	contamination similar to CIC, possible hydraulic fluid		√
		6B	contamination similar to CIC, possible hydraulic fluid	√	√
		6C	film id'ed as PET, contamination similar to CIC	√	
411U4120-4606	7	7A	film id'ed as PET		
		7B	Small area pink contaminate/stain id'ed as dye		
		7C	see Table II		

Particulate Contamination:

Particulate contamination was identified by visual inspection using bright field optical microscopy and polarized light microscopy (PLM). Fibrous matter was identified using PLM and index of refraction oils. Fibrous matter was identified as dyed synthetic red, blue, green fibers, dyed cellulose (cotton fibers) and paper like cellulose, also fiberglass similar to blanket insulation and bundles of fiberglass not similar to blanket insulation were found. The particulate matter included: general dust, animal hair (some 4-6" long), cellulose fibers, mineral particles, Styrofoam, metal fragments, insects, and CIC flakes (identified by FTIR and EMPA). Examples of particulate contamination can be seen in Figure 7.

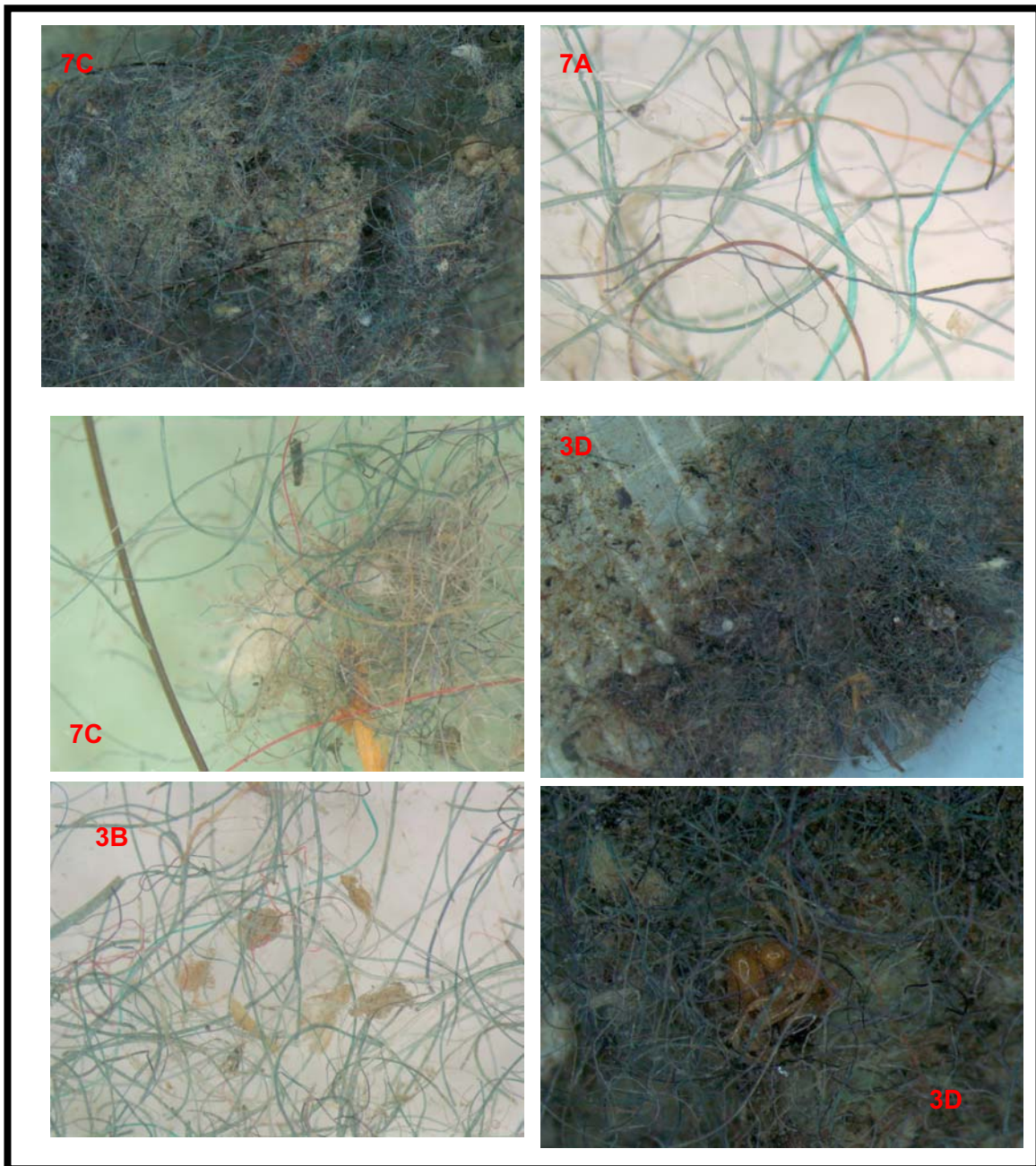


Figure 7: Particulate and Fibrous Particulate and Fibrous Surface Contamination, showing overall view and fibers dispersed view.

Summary of Results: Table II

Particulate Contamination			
Part #	Blanket	Sample	Summary of Results
411U4055-1037	1	1A	No obvious particulates
		1B	No obvious particulates
411U4120-2386	2	2A	No obvious particulates
		2B	No obvious particulates
411U4120-2702	3	3A	general dust*, fibers**, animal hair (some 4-6" long) , cellulose fibers, mineral particles, Styrofoam, metal fragments
		3B	general dust, fibers, animal hair, cellulose fibers, mineral particles, plastic, Styrofoam, metal fragments
		3C	general dust, fibers, mineral particles, CIC particles
		3D	general dust, fibers, animal hair, cellulose fibers, mineral particles, CIC particles, insects
61B50025-1002	4		No sample received for this number
411U4120-2383	5	5A	No obvious particulates
411U4120-4302	6	6A	general dust, fibers, mineral particles, CIC particles
		6B	general dust, fibers, mineral particles, CIC particles
		6C	general dust, fibers, mineral particles, CIC particles
411U4120-4606	7	7A	general dust, fibers, animal hair, cellulose fibers, mineral particles, metal fragments
		7B	general dust, fibers, animal hair, cellulose fibers, mineral particles, seed, wood chip
		7C	general dust, fibers, animal hair, cellulose fibers, mineral particles, plastic, piece of sealant

* **Fibers include: dyed synthetic red, blue, green fibers, dyed cellulose (cotton fibers) and paper like cellulose, also fiberglass similar to blanket insulation and bundles of fiberglass**

****General dust includes fine mineral particles, calcium carbonate, calcium sulfonate, and sodium chloride particles**

CONCLUSION:

The insulation blanket film was characterized as similar to Polyethylene Terephthalate reference materials. The surface contamination was consistent with corrosion inhibiting compound. Particulate matter was made up of synthetic and natural fibers, animal hair, cellulose fibers, mineral particles, plastic, Styrofoam, metal fragments, and insects.

References:

- a) BMS8-142
- b) M&PT Standard Bulletin: Standard Guide for Identification of ORCON Orcofilm® AN-26 and AN-36W Adhesives by Infrared Spectroscopy
- c) WR200802155-S00
- d) WR200802155-S01